# SEE FOLLOWING NOTE

☐ **PLEASE NOTE THAT PAGINATION APPEARS IRREGULAR, BUT THE TEXT IS COMPLETE.**

☑ THIS DOCUMENT MAY BE INCOMPLETE OR PARTLY ILLEGIBLE. NO BETTER COPIES ARE AVAILABLE, MICROMEDIA HAS DECIDED TO FILM THE DOCUMENT FOR ARCHIVAL PURPOSES

---

# VOIR NOTE CI-APRÉS

☐ VEUILLEZ NOTER QUE LA PAGINATION EST ERRONEÉ MAIS LE TEXTE EST INTÉGRAL.

☑ CE DOCUMENT N'EST PAS COMPLETE ET/OU EST EN PARTIE ILLISIBLE. MEILLEURS COPIES N'EXISTENT PAS DONC MICROMEDIA A DECIDE DE FILMER LE DOCUMENT POUR LES BESOINS DES ARCHIVES.

Micromedia
ProQuest

20 Victoria Street
Toronto, Ontario M5C 2N8
tel: (416) 362-5211
toll free: 1-800-387-2689
fax: (416) 362-6161
web: www.micromedia.ca

P518202.PDF [Page: 3 of 49]

Copy No. 21

DEFENCE R&D DÉFENSE

# Evaluation of the Transition Properties of CSA 350WT and Modifying the DREA Instrumented Impact Testing System

*K.J. KarisAllen*

*FACTS Engineering Inc.*
*P.O. Box 20039*
*Halifax, Nova Scotia*
*Canada B3R 2K9*

*Contract Number: W7707-00-8893/001/HAL*
*Contract Scientific Authority: Dr. James R. Matthews*
*Phone Number: (902) 727 0550 ext 3444*

**Defence R&D Canada**

Contractor Report
DREA CR 2002-006
January 2002

National Defence Défense nationale

Canada

P518202.PDF [Page: 4 of 49]

104-06916/

Copy No: _____.

# Evaluation of the Transition Properties of CSA 350WT and Modifying the DREA Instrumented Impact Testing System

K.J. KarisAllen

FACTS Engineering Inc.
P.O. Box 20039
Halifax, Nova Scotia
Canada, B3R 2K9

Contract Number: W7707-00-8893/001/HAL
Contract Scientific Authority: Dr. James R. Matthews
Phone Number: (902) 727 0550 ext 3444

**Defence Research Establishment Atlantic**

Contractor Report

DREA CR 2002-006

January 2002

Approved by

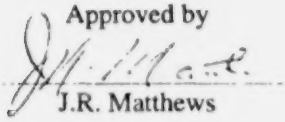

J.R. Matthews

Scientific Authority

Approved for release by

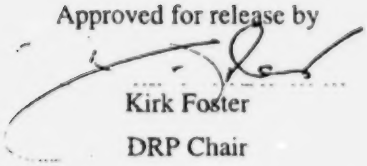

Kirk Foster

DRP Chair

The scientific or technical validity of this Contract Report is entirely the responsibility of the contractor and the contents do not necessarily have the approval or endorsement of Defence R&D Canada

© Her Majesty the Queen as represented by the Minister of National Defence, 2002

© Sa majesté la reine, représentée par le ministre de la Défense nationale, 2002

## Abstract

Energy based temperature transition curves have been constructed for a CSA G40.21 350WT structural steel for several specimen geometries using the load-displacement data generated by an instrumented impact test system. Specimen geometries employed include standard pressed notched ASTM E-604 and ASTM E-604 specimens precracked to approximately 0.55 a/W with notch orientations in both the T-L and L-T orientation. The effects of machining side grooves into the lateral specimen faces for both notch geometries has also been evaluated. A framework for adjusting material temperature transition curves has been described. The framework proposed focuses on the adjustment of the transition temperature owing to conversion of plastic strain energy in the crack tip plastic zone into heat.

The results indicate that with the exception of the pressed-notched, side-grooved specimens, the data from the lower shelf (brittle) to the upper shelf (ductile) combine to generate typical transition curve morphologies. Visual examination of the fracture surfaces of the pressed-notched, side-grooved specimens revealed significant amounts of out of plane fracture. The out of plane fracture morphology observed for the side-grooved pressed-notch specimens has been attributed to the fracture event initiating at the specimen lateral surfaces . It was observed that within a specific specimen geometry, both T-L and L-T notch orientations produced similar transition temperatures. The transition temperatures predicted by the non-side-grooved precracked and non-side-grooved pressed-notch geometries were approximately -15°C and -25°C respectively. These results indicated a small geometry dependence of the lower knee transition temperature of approximately 10°C between these two geometries.

Lower knee load-displacement records were used to analyse the magnitude of the temperature adjustment for both the precracked and pressed notch L-T 350 WT steel specimens. The analysis indicated that the predicted geometry independent material transition temperature is -13.7°C and -13.5°C for the ASTM E-604 pressed notch and precracked specimen, respectively. While the analysis conducted into the validity of this framework is by no means exhaustive, the agreement between the material transition temperature as predicted by the two specimen geometries employed warrants further study

?518202 PDF [Page: 7 of 49]

## Résumé

À partir de données charge-déplacement obtenues à l'aide d'un système d'essai de résistance au choc, on a déterminé les courbes de transition thermique, basées sur l'énergie, d'éprouvettes d'acier profilé CSA G40.21 350WT présentant plusieurs géométries. Parmi les géométries utilisées, on compte des éprouvettes standard ASTM E-604 qui ont été embouties et entaillées et des éprouvettes ASTM E-604 préfissurées à environ 0,55 a/W, avec des orientations d'entaille T-L et L-T. On a aussi évalué les effets de rainures latérales réalisées par usinage sur les côtés des éprouvettes pour les deux géométries d'entaille. On décrit une méthode permettant d'ajuster les courbes de transition thermique du matériau. La méthode proposée consiste principalement à ajuster la température de transition découlant de la conversion en chaleur de l'énergie de déformation plastique dans la zone plastique en tête de fissure.

Sauf dans le cas des éprouvettes embouties et entaillées présentant des rainures latérales, les résultats obtenus indiquent que les données comprises entre le plateau inférieur (matériau cassant) et le plateau supérieur (matériau ductile) se combinent pour donner des courbes de transition de forme typique. L'examen visuel des surfaces de fracture des éprouvettes embouties et entaillées à rainures latérales a révélé la présence d'un nombre assez important de fractures hors plan. La morphologie des fractures hors plan observées dans les éprouvettes embouties et entaillées à rainures latérales a été attribuée au processus de fracture qui commence sur les surfaces latérales des éprouvettes. On a observé que, pour une géométrie particulière d'éprouvette, les orientations d'entaille T-L et L-T produisent l'une et l'autre des températures de transition similaires. Les températures de transition prévues pour les géométries préfissurées mais sans rainure latérale et pour les géométries embouties et entaillées mais sans rainure latérale étaient respectivement d'environ – 15 °C et – 25 °C. Ces résultats indiquent qu'il existe entre ces deux géométries une légère dépendance sur le coude inférieur de la courbe de température de transition à environ 10 °C.

On a utilisé des données charge-déplacement dans la zone du coude inférieur de la courbe pour analyser l'importance de l'ajustement de température pour les éprouvettes en acier 350 WT préfissurées et les éprouvettes embouties et entaillées avec une orientation d'entailles L-T. Cette analyse indique que les valeurs prévues pour la température de transition indépendante de la géométrie sont de – 13,7 °C et – 13,5 °C pour les éprouvettes ASTM E-604 embouties et entaillées et préfissurées, respectivement. L'analyse portant sur la validité de cette méthode n'est nullement exhaustive, mais la concordance des températures de transition prévues pour les deux géométries d'éprouvette utilisées justifie l'exécution d'études ultérieures

## Executive summary

The DREA Drop Weight Impact Test Facility Instrumentation has been upgraded and new faster boards installed. This makes this system easier to operate and improves the usefulness of the various components. Copies of the instrumentation have been received and stored for backup and computer replacement in future. The report contains a working users manual in the appendix.

Using the new instrumentation, energy based temperature transition curves have been constructed for a CSA G40.21 350WT structural steel for several specimen geometries using the load-displacement data generated by the software. Specimen geometries employed include standard pressed notched ASTM E-604 specimens as well as ASTM E-604 specimens precracked to approximately 0.55 a/W with notch orientations in both the T-L and L-T orientation. The effects of machining side grooves into the lateral specimen faces for both notch geometries has been evaluated

A framework for adjusting material temperature transition curves has been described The framework proposed focuses on the adjustment of the transition temperature owing to conversion of plastic strain energy in the crack tip plastic zone into heat This causes the effective test temperature to rise more for notched specimens than precracked specimens explaining the shift in their respective transition curves.

The results indicate that with the exception of the pressed-notched, side-grooved specimens, the data from the lower shelf (brittle) to the upper shelf (ductile) combine to generate typical transition curve morphologies.

Visual examination of the fracture surfaces of the pressed-notched, side-grooved specimens revealed significant amounts of out of plane fracture. The out of plane fracture morphology observed for the side-grooved pressed-notch specimens has been attributed to the fracture event initiating at the specimen lateral surfaces. This also explains their apparent two mode results. When the fracture initiation changes from the edge to the center the mode changes.

KarisAllen, K.J.. 2002. Evaluation of the Transition Properties of CSA 350WT and Modifying the DREA Instrumented Impact Testing System. DREA CR 2002-006 Defence Research Establishment Atlantic.

P518202.PDF [Page: 9 of 49]

## Sommaire

Les appareils de l'installation d'essai de la résistance au choc par chute de poids du CRDA ont été modernisés et de nouvelles cartes plus rapides ont été installées. Ce système est maintenant plus facile à utiliser et ses divers éléments sont plus utiles. On a reçu des cartes supplémentaires qui ont été entreposées; elles serviront de cartes de secours et seront également utilisées lors du remplacement des ordinateurs. Le rapport renferme en annexe un manuel destiné aux utilisateurs.

Grâce aux nouveaux appareils, on a déterminé, à partir de données charge-déplacement obtenues à l'aide d'un logiciel, les courbes de transition thermique, basées sur l'énergie, d'éprouvettes d'acier profilé CSA G40.21 350WT présentant plusieurs géométries. Parmi les géométries utilisées, on compte des éprouvettes standard ASTM E-604 qui ont été embouties et entaillées ainsi que des éprouvettes ASTM E-604 préfissurées à environ 0,55 a/W, avec des orientations d'entaille T-L et L-T. On a aussi évalué les effets de rainures latérales réalisées par usinage sur les côtés des éprouvettes pour les deux géométries d'entaille.

On décrit une méthode permettant d'ajuster les courbes de transition thermique du matériau. La méthode proposée consiste principalement à ajuster la température de transition découlant de la conversion en chaleur de l'énergie de déformation plastique dans la zone plastique en tête de fissure. Cette conversion provoque, dans les éprouvettes entaillées, une hausse de la température effective d'essai plus importante que dans les éprouvettes préfissurées, ce qui explique le décalage observé dans leurs courbes de transition respectives.

Sauf dans le cas des éprouvettes embouties et entaillées présentant des rainures latérales, les résultats obtenus indiquent que les données comprises entre le plateau inférieur (matériau cassant) et le plateau supérieur (matériau ductile) se combinent pour donner des courbes de transition de forme typique.

L'examen visuel des surfaces de fracture des éprouvettes embouties et entaillées à rainures latérales a révélé la présence d'un nombre assez important de fractures hors plan. La morphologie des fractures hors plan observées dans les éprouvettes embouties et entaillées à rainures latérales a été attribuée au processus de fracture qui commence sur les surfaces latérales des éprouvettes, ce qui permet aussi d'expliquer leurs résultats apparents à deux modes. Le mode change lorsque la fracture commence et se propage à partir du côté vers le centre.

KarisAllen, K.J. 2002. Evaluation of the Transition Properties of CSA 350WT and Modifying the DREA Instrumented Impact Testing System. DREA CR 2002-006 Defence Research Establishment Atlantic.

# Table of contents


Abstract i

Résumé ii

Executive summary iii

Sommaire iv

Table of contents v

List of figures vii

1.0 Introduction 1
2.0 Background
2.1 Qualitative Test Procedures 2
2.2 Transition Temperature and Specimen Geometry 3
2.3 Generating and Interpreting Instrumented Load/Displacement Data 4
3.0 Experimental Program
3.1 Specimen Preparation 7
3.2 Impact Instrumentation and Test Procedure 7
4.0 Results
4.1 Analysis of the Instrumented Load Displacement Record 8
4.2 Transition Curve Test Results 10
5.0 Discussion 15
6.0 Conclusions 17
7.0 References 18

Appendix A - DREA Instrumented Impact Test System 19
A 1.0 System Description
A.1.1 Hardware Requirements 20
A.1.2 Software Requirements 21
A.1.3 Calibration Procedure 21
A.2.0 Getting Started 24
A.2.1 Inputting Test Variable Parameters 25
A 2 2 Data Capture and Post Processing 26
A.2.3 Viewing Waveform Data 26
A.2.4 Saving and Printing Data 27
A.3.0 Experimental Verification of Instrumentation 27
A.4.0 File Structures
A.4 1 Digitized Load/Time File 29
A.4.2 Load/Displacement File 30
A.5 0 Calibration Data
A.5.1 Range 5VDC-X10 31

P518202.PDF [Page: 11 of 49]

A.5.2 Range 1VDC-X100 31
A.5.3 Range 2.7VDC-X100 32
A.5.4 Range 5VDC-X100 32

## List of figures

Figure 2.1. Schematic representation of an instrumented impact load-displacement record 5

Figure 4.1 Instrumented load-displacement record for a 350WT specimen tested at -15 C. 9

Figure 4.2 Instrumented load-displacement record for a 350WT specimen tested at -30 C. 9

Figure 4. Temperature transition curve for standard ASTM E-604 specimens. The notch was oriented in the L-T direction and the notch tip was pressed in accordance with ASTM E-604. 11

Figure 5. Temperature transition curve for standard ASTM E-604 specimens. The notch was oriented in the L-T direction and the notch tip was pressed in accordance with ASTM E-604. 11

Figure 6. Temperature transition curve for standard ASTM E-604 specimens with a 20 percent of the thickness side groove. The notch was oriented in the L-T direction and the notch tip was pressed in accordance with ASTM E-604. 12

Figure 7. Temperature transition curve for standard ASTM E-604 specimens with a 20 percent of the thickness side groove. The notch was oriented in the T-L direction and the notch tip was pressed in accordance with ASTM E-604. 12

Figure 8 Temperature transition curve for standard ASTM E-604 specimens precracked to .54 a/W with the notch oriented in the L-T orientation. 13

Figure 9 Temperature transition curve for standard ASTM E-604 specimens precracked to .54 a/W with the notch oriented in the T-L orientation. 13

Figure 10. Transition data curve for ASTM E-604 specimens side grooved to 20 percent of the specimen thickness and precracked to .54 a/W. The notch for these specimens was machined in the L-T orientation. 14

Figure 11. Transition data curve for ASTM E-604 specimens side grooved to 20 percent of the specimen thickness and precracked to .54 a/W. The notch for these specimens was machined in the T-L orientation. 14

## List of tables

Table 4.1. Transition temperatures for the eight specimen geometries evaluated 10

P518202.PDF [Page: 13 of 49]

## 1.0 INTRODUCTION

In the past five to ten years, the commercial shipping industry has recorded an increase in structural fracture failures. This increase has led to the development of knowledge pertaining to the fracture mechanisms relevant to the ductile to brittle transition region. To some extent, the increase in failure incidents can be attributed to a combination of longer periods between scheduled maintenance and the absence of a rigorous damage tolerance assessment of the construction materials during the design stage of these structures.

Recently, the Canadian Navy added twelve "Halifax Class" patrol frigates (CPF) to its fleet. The global design stresses in these structures under operational service conditions were increased over previous military designs. Also, in an effort to reduce life-cycle maintenance costs, fleet maintenance facilities are implementing dockside inspection and maintenance to increase the periods between the more rigorous refit maintenance cycles. Responding to these changes, the defence research and development community has initiated both in-house and contracted programs to ensure that these structures maintain an acceptable level of damage tolerance for the assigned operational envelop.

Accurate characterization of mechanical material properties is integral to the development of marine platform designs which will exhibit acceptable levels of damage tolerance under extreme service conditions. Currently, structural steels and welds comprise the bulk of materials used to fabricate marine platforms. Fracture mechanics is a mechanical/materials discipline which evolved to provide designers with information critical to the longevity and safe service performance of structures which contain defects. It is the study of the interaction between defects, applied stress, geometry, and materials properties. Defects can be formed during the material processing stage (rolling laminations), during fabrication of the structure (weld defects) or formed as a result of the in service stresses and strains applied to the structure (fatigue cracking). Cracks will continue to grow by subcritical mechanisms until they reach a critical length at which point they will initiate and propagate. These cracks can propagate under limit state conditions either by ductile tearing, where the mechanism is dominated by microvoid coalescence, or by brittle propagation, which is dominated by transgranular cleavage. Which mechanism dominates is determined by variables such as temperature, strain rate, and defect constraint.

## 2.0 BACKGROUND

### 2.1 Qualitative Test Procedures

Several test procedures have been incorporated into standardized test methods for the development of temperature transition curves. The most commonly used procedure is ASTM E-23 [1], which is commonly referred to as the Charpy V-notch test method. The Charpy V-notch procedure is a dynamic test which uses a 10 mm x 10 mm x 55 mm bend bar with a shallow 2 mm deep machined notch. The root tip radius of this notch is 0.25 mm. The energy required to fracture the specimens is recorded for various temperatures. This data is used to generate a temperature transition curve.

The dynamic tear test developed by US naval researchers was standardized into ASTM E-604 [2]. The E-604 specimen is significantly larger than the E-23 specimen (16 mm x 40.62 mm x 181mm) and provides increased lateral and back face constraint as compared to the E-23 specimen. The 12 mm notch in this specimen is pressed with a hardened knife to increase the crack tip stress intensity factor. Similar to the E-23 test method, the fracture energy required to fail the specimen at various temperatures is used as the data for developing the material transition curve.

Drop-weight tear testing of ferritic steels (ASTM E-436 [3]) provides a visual method for determining the transition behaviour of materials. A 75 mm x 300 mm specimen by the as received thickness of the plate is impacted at dynamic loading rates. A shallow pressed-notch is created on the tension surface to initiate the fracture event. The standard uses the percent area of cleavage fracture to determine the transition characteristics of a material.

The specimen configuration of the nil ductility test method (ASTM E-208 [4]) is substantially different than the above described test methods. The specimen thickness to height of this specimen is 3.5/1 (in all the above procedures, the thickness to height is less than 1/1). This specimen incorporates a brittle starter notch to initiate the fracture. As opposed to getting a complete transition curve, this test method is used to define the nil ductility temperature (NDT) at which complete lateral cracking occurs across the specimen.

A relatively recent unstandardized test procedure for the generation of transition curves is the measurement of the residual shear lip created by the fracture process [5,6 ]. The specimen geometry used is the same as in ASTM E-604. Numerous studies have shown that the shear lip width correlates well to fracture energy. Intuitively, shear lip width should also correlate well with crack arrest toughness, $K_a$, since it is measured at a point on the fracture surface where a brittle crack is dominating the fracture process. This test has the added advantage that it does not require the expensive instrumentation of tests such as E-604.

## 2.2 Transition Temperature and Specimen Geometry

Section 2.1 summarized several standardized and non-standardized qualitative test procedures available for determining material transition behaviour. The overall objective of choosing which procedure to employ resides in their ability to accurately predict structural material response under similar conditions between the laboratory and the field. The test procedures described above produce transition curves information which may differ significantly. Research has shown [7] that a significant predicted transition temperature shift can occur when comparing the dynamic tear energy transition to Charpy V-notch energy transition data. The lower transition temperature generated by the Charpy V-notch specimens has been historically attributed to the lack of specimen capacity of the Charpy specimen owing to specimen size and notch acuity differences.

The basic information required from a transition curve analysis is the temperature at which the material microstructure becomes susceptible to transgranular cleavage. A subject area which has received very little attention and which may contribute significantly to the position of the predicted temperature transition is the incorporation into the analysis of the effects of material temperature change owing to the effects of crack tip plasticity. During an impact test, the majority of the energy absorbed by the specimen is either elastic energy (which is recoverable) and plastic energy (which is non recoverable). It has been postulated [8] that between 90-100 percent of the plastic energy absorbed by the specimen is converted into heat. In a previous study [9] into the transition behaviour of CSA 350 WT, uniaxial tension specimens were conditioned to a pretest temperature of -50°C. Immediate post test examination of the specimens revealed that the frost buildup on the majority of the specimens was liquid over the portion of the gauge length which sustained significant plasticity (indicating a material temperature shift of at least 50°C over the duration of the test). The final fracture was dominated with microviod coalescence even though the dynamic tear transition curve indicated a ductile-brittle transition of approximately -25°C for this material.

During an impact test of a notched or precracked specimen, the majority of the plastic strain sustained by the specimen is localized in the plastic zone around the tip of the notch . The distribution and magnitude of the stress fields around the crack tip are critically dependent on both notch tip acuity and the plastic flow properties of the material. Specimen geometries such as the Charpy V-notch specimen with a relatively blunt notch will generate a significantly larger plastic zone ahead of the notch as compared to the relatively more acute notch incorporated into specimens such as the ASTM E-604 specimen geometry. Since this notch tip plasticity is converted into heat, a blunt notch will result in a larger zone of temperature increase as compared to a more acute notch. In order to initiate a transgranular cleavage fracture, two primary conditions must occur simultaneously. First, the microstructure must be susceptible which in this case is governed by the crack tip material temperature. Secondly, a minimum critical stress level must be achieved over a critical volume in advance of the notch. If microstructure susceptibility is governed by temperature it could be postulated that a substantial portion of the differences in transition temperatures observed between differing specimen notch tip geometries results from differences in crack tip heating.

P518202.PDF [Page: 16 of 49]

## 2.3 Generating and Interpreting Instrumented Load/Displacement Data

The majority of commercially available instrumented impact test systems record the signal produced from a force transducer located in the striker with respect to time. Specimen load line displacement is determined indirectly using the force transducer signal combined with conservation of energy principles [10-12]. To convert force-time data to force-displacement data the velocity over the entire impact test must be accurately determined. If system friction is assumed to be negligible, the initial impact velocity ($V_o$) may be calculated from the initial height of the hammer assembly as:

$$V_o = \sqrt{2\,g\,h_o} \tag{2.1}$$

where (g) is the acceleration due to gravity and (h) is the initial height of the hammer. As the specimen is contacted, there is a loss of energy and an associated loss of velocity, as follows:

$$m\int V\,d\,V + m\,g\int d\,h - \int P_a V_a d = 0 \tag{2.2}$$

where (m) is the mass of the hammer, (V) is the the instantaneous velocity, and (P) is the specimen loading response. The energy absorbed by the specimen (represented by the third term) is approximated by the area from time i to i+1 under the force time curve multiplied by the average velocity from time i to i+1. The second term calculates the potential energy converted to kinetic energy due to vertical displacement of the striker assembly. In this manner, the velocity can be calculated for all times and the time can be converted to displacement by continually dividing time increments by the average calculated velocity during these periods.

Fundamental to the interpretation of the temperature transition curve generated from instrumented impact test systems is a detailed understanding of the specimen mechanical response during the impact event. Figure 2.1 is a schematic representation of the typical mechanical (load/displacement) response of a single edge-notched specimen during a three-point bending impact event. Previous studies conducted [13,14] indicate that time t=0 s for a specimen initially at rest on the anvils (V=0 m/s) the initial loading response of the specimen as measured by a force transducer located in the striker is dominated by the transfer of inertial energy to the specimen in order to increase the specimen load line deflection rate to the velocity of the striker (Zone 1). Evidence also indicates [13] that for short inertial energy transfer periods, the mechanical response of the specimen is essentially single point bending (specimen rotates off the

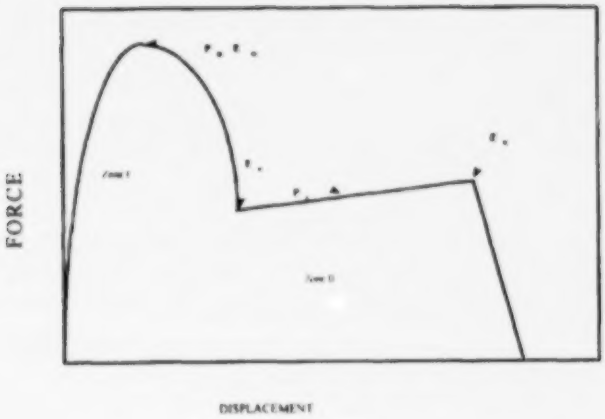


**Figure 2.1** - Schematic representation of an instrumented impact load-displacement record.

anvils without any evidence of a reaction force). The peak force generated during this inertial transfer of energy can be verified using:

$$F = m_e a \tag{2.3}$$

where ($m_e$) is the effective mass of the specimen (approximated as ½ the actual mass of a specimen rotating with respect to the load line) and (a) is the average acceleration of the specimen which can be calculated from:

$$a = \frac{v_s}{t_p} \tag{2.4}$$

where ($v_s$) is the initial impact velocity of the striker and ($t_p$) is the time increment from initial impact to peak inertial loading as determined from the instrumented load time trace. The associated energy transferred to the specimen to peak loading ($E_p$) may also be verified using:

$$E_p = \frac{1}{2} m_e v_s^2 \tag{2.5}$$

As the specimen ends rotate back towards the anvils, the transfer of inertial energy continues until the ends recontact the anvil supports. Once the specimen ends recontact the anvil supports, the mechanical loading response of the specimen is governed by the elastic and elastic-plastic three-point deflection characteristics of the specimen (Zone 2). Maximin sustainable load can be approximated using relationships such as those published in ASTM E1152 [15] which is given as:

$$P_L = \left[\left(\frac{4}{3}\right)\left(\frac{B b_o^2 \sigma Y}{S}\right)\right] \qquad (2.6)$$

where (B) is the specimen thickness, ($b_o$) is the remaining uncracked ligament, (S) is the anvil span and ($\sigma_Y$)is the effective flow stress of the material.

The current program focuses on the ability of the dynamic tear (E-604) specimen geometry with a pressed-notch to accurately reflect structural material performance. Instrumented impact dynamic tear transition curves will be compared to transition curves generated from fatigue precracked specimens. The effects of the modification of through thickness lateral constraint as the result of side-grooving the specimens will also be studied.

## 3.0 EXPERIMENTAL PROGRAM

### 3.1 Specimen Preparation

Ninety specimens were machined from 12.5 mm CSA G40.21 350WT material supplied by DREA/DL. Two sets of forty-five specimens each were fabricated from the plates such that the plate rolling direction with respect to the crack orientation conformed to the T-L and L-T orientations as specified in ASTM E-399 [16]. Twelve mm notches were machined into twenty-five specimens from each set of forty-five specimens. Fifteen specimens from each set of twenty specimens were side grooved to 20 percent of the specimen thickness. All fifty specimens were subsequently pressed with a notch sharpening knife edge blade in accordance with ASTM E-604. The remaining forty specimens were machine notched to a depth of 18 mm. Side-grooves of 20 percent of the thickness were machined into ten specimens each from the T-L and L-T orientations. The notches of these forty specimens were precompressed to 40 percent of the limit load as defined by ASTM E-1152 and subsequently fatigue precracked to a depth of approximately .55 a/W using an R ratio of 0.1 and a maximum stress intensity factor of 30 MPa$\sqrt{m}$.

### 3.2 Impact Instrumentation and Test Procedure

In a previous study [10], a PC based software/hardware suite was developed. The suite was configured around a single screen virtual instrument which controlled the capture and analysis of instrumented force/time data. Algorithms for data storage and the conversion of force/time to force displacement were included to provide the user with the ability to conduct testing from data capture through energy calculation in a single software package. Several modifications have been incorporated into the software to increase its flexibility and reliability. A user manual describing the hardware/software specifications and detailing the functional use of the software interface is provided in Appendix A.

Specimens were tested at impact loading rates of approximately 5.4 m/s with a 275 kg crosshead. Prior to testing, specimens were conditioned to various temperatures ranging over the ductile-brittle transition of this material using a fluid cold bath. Analog impact signals generated from an instrumented tup were digitized using an 8 bit A/D converter and stored in a microprocessor for further analysis. Force-time information was converted into force displacement using conservation of energy principles for each specimen. Impact energy for each specimen was determined by integration of the force-displacement data.

## 4.0 RESULTS

### 4.1 Analysis of the Instrumented Load/Displacement Record

Figure 4.1 shows typical lower shelf instrumented impact test records for a specimen precracked in the L-T orientation (without side grooves) tested at -15°C (lower transition knee). As evidenced by the load/displacement record, the impact inertial energy impulse dominates the initial specimen loading response. The peak loading for this impulse and the absorbed energy at peak loading as determined from the load displacement trace are given as approximately 92 kN and 4.0 J, respectively. The time interval between initial impact and peak load is given as 18 μs. Given an initial impact velocity of 5.4 m/s, the average acceleration to peak loading can be calculated as approximately 300000 m/s$^2$ (equation 2.4). Based on a material density of 8 g/cm$^3$, the total mass of the specimen can be approximated as 0.66 kg. Using equations 2.3 and 2.5, the theoretical load and absorbed energy to peak inertial loading are given as 99 kN and 4.8 J, respectively. Thus the measured inertial loading absorbed energy are in good agreement with the calculated theoretical magnitudes. Similar to the peak energy, the measured total inertial impulse energy of 8.1 J is in good agreement with the calculated theoretical total impulse energy 9.6 J. Subsequent to the inertial loading impulse, the load displacement record exhibits a relatively flat loading section. It has been postulated that the loading in this section should be characterized by the plastic flow properties of a precracked specimen. Using equation 2.6 combined with the average load in this portion of the trace (19 kN), the material flow stress is calculated as 550 MPa. The calculated flow stress is consistant with that expected for this material under dynamic loading rates.

Figure 4.2 shows typical lower shelf transition knee instrumented impact test records for a ASTM E-604 specimen with a pressed notch in the L-T orientation (without side grooves) tested at -30°C (lower transition knee). Similar to the precracked specimen, the impact inertial energy impulse dominates the initial specimen loading response. The measured impulse peak load, peak energy and total energy for this test are given as 94.4 kN, 4.0 J, and 8.0 J, respectively. Again, similar to the precracked specimen, the measured values are in good agreement with the calculated theoretical values ( the calculated values are the same as the previous specimen). The post impulse flat section of the record indicates a measured average load of 40 kN. Using equation 2.6 this loading indicates a material flow stress of 500 MPa. Again, the calculated flow stress is consistant with that expected for this material under dynamic loading rates.

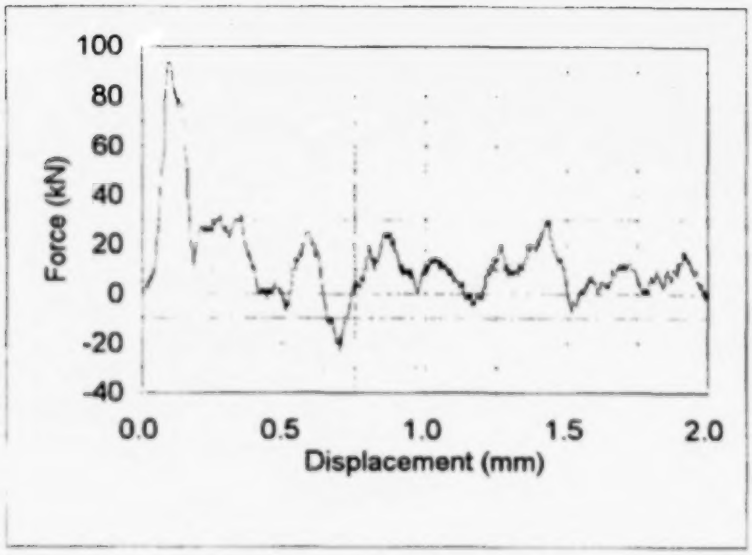


**Figure 4.1** - Instrumented load-displacement record for a 350WT specimen tested at -15 °C (notch configuration - precracked to 0.55 a/W, notch orientation - L-T)

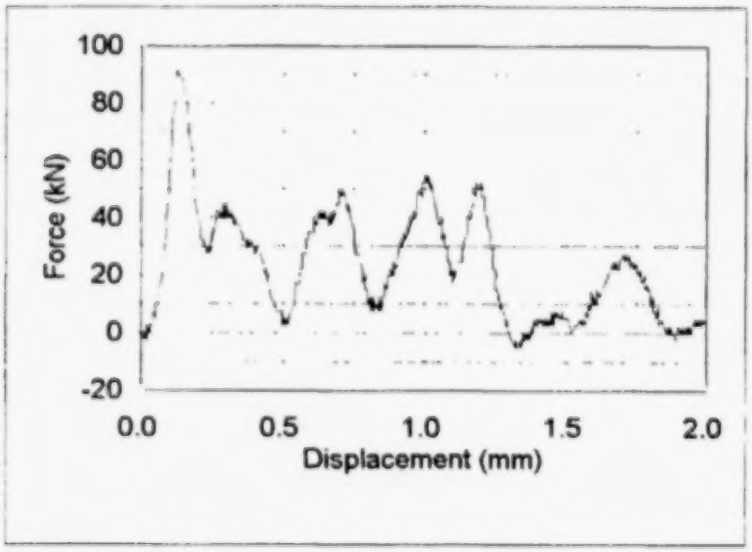


**Figure 4.2** - Instrumented load-displacement record for a 350WT specimen tested at -30 °C (notch configuration - pressed notch ASTM E-604, notch orientation - L-T)

## 4.2 Transition Curve Test Results

Figures 4.3 - 4.10 represent the total energy absorbed temperature transition curves for the eight specimen configurations tested. With the exception of the pressed-notched, side-grooved specimens, the data from the lower shelf (brittle) to the upper shelf (ductile) combine to generate typical transition curve morphologies. Visual examination of the fracture surfaces of the pressed-notched, side-grooved specimens revealed significant amounts of out of plane fracture. The reasons for the differing transition curve and fracture surface morphology will be explored further in the discussion of the results.

Table 4.1 summarizes the lower knee transition temperatures results determined from the eight specimen configurations tested. For the pressed-notch, non side-grooved specimens tested, the transition temperatures are -25°C for notch orientations in the L-T and T-L orientations. For the pressed-notched, side-grooved specimens, the lower knee transition temperature was determined to be approximately -35°C for both the L-T and T-L orientations, respectively. The lower knee transition temperature for the precracked non side grooved specimens were -17°C and -15°C for the notch orientations in the L-T and T-L orientations, respectively. For the precracked side-grooved specimens, the lower knee transition temperatures were determined as -8°C and -15°C for the L-T and T-L notch orientations, respectively. In general, it was observed that for a given specimen and notch geometry, the transition temperature as determined from the total absorbed energy is similar for both the L-T and T-L orientations. Also, except for the precracked side-grooved specimens, within given specimen geometry, the magnitude of the lower shelf and upper shelf absorbed energies for the L-T orientation is only slightly elevated over the T-L orientation (L-T/T-L energy ratios remain below 1.3/1). For the precracked side-grooved specimens, the absorbed energy for upper shelf fracture is approximately 1.7/1. A comparison of the upper shelf absorbed energies between the pressed-notch and the fatigue precracked specimens indicates an upper shelf absorbed energy ratio of approximately 2/1 in favour of the pressed notch specimens.

**Table 4.1** - Transition temperatures for the eight specimen geometries evaluated.

| | Notch Orientation | | | | | | | |
|---|---|---|---|---|---|---|---|---|
| | T-L | | | | L-T | | | |
| | PC | PC-SG | DT | DT-SG | PC | PC-SG | DT | DT-SG |
| Teansition Temperature (°C) | -15 | -15 | -25 | -35 | -17 | -8 | -25 | -35 |

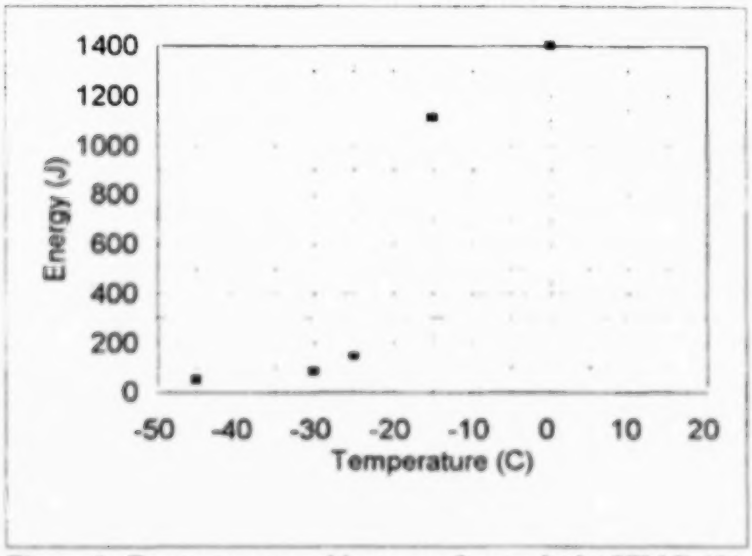


**Figure 4** - Temperature transition curve for standard ASTM E-604 specimens. The notch was oriented in the L-T direction and the notch tip was pressed in accordance with ASTM E-604.

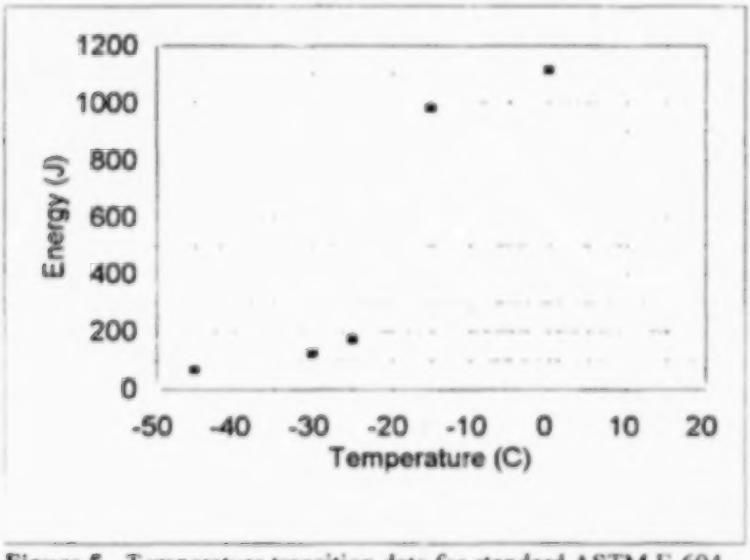


**Figure 5** - Temperature transition data for standard ASTM E-604 specimens. The notch was oriented in the T-L direction and the notch tip was pressed in accordance with ASTM E-604.

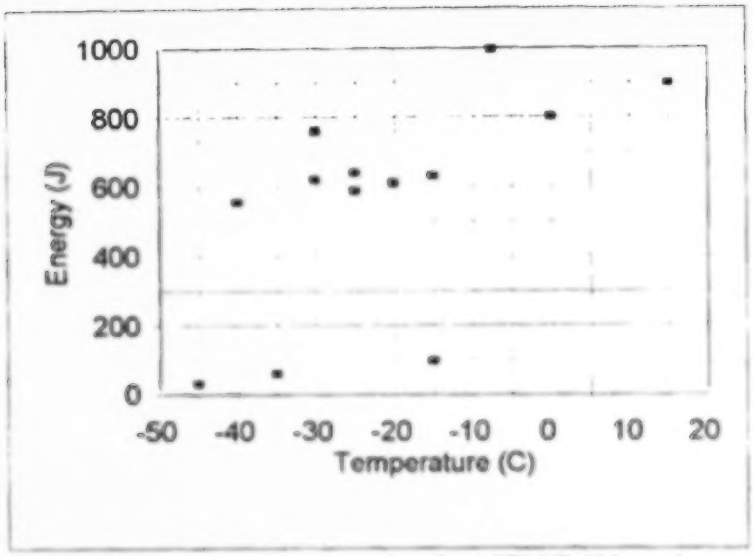


**Figure 6**- Temperature transition data for ASTM E-604 specimens with a 20 percent of the thickness side groove. The notch was oriented in the L-T direction and the notch tip was pressed in accordance with ASTM E-604.

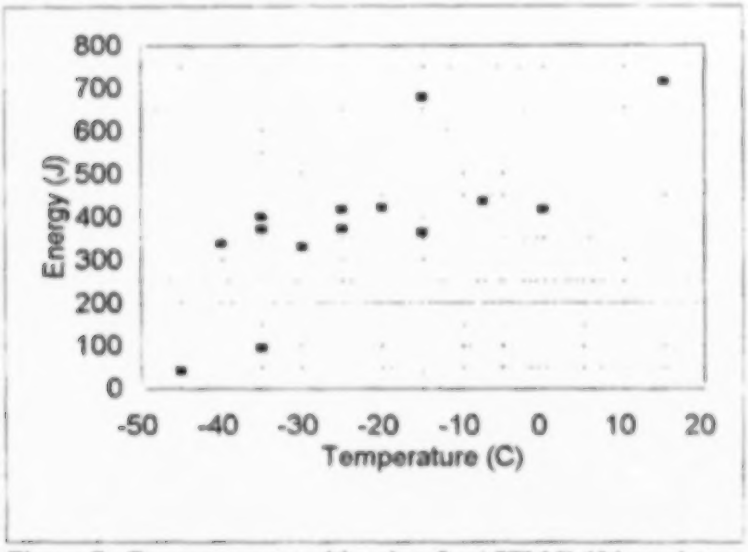


**Figure 7** - Temperature transition data for ASTM E-604 specimens with a 20 percent of the thickness side groove. The notch was oriented in the T-L direction and the notch tip was pressed in accordance with ASTM E-604.

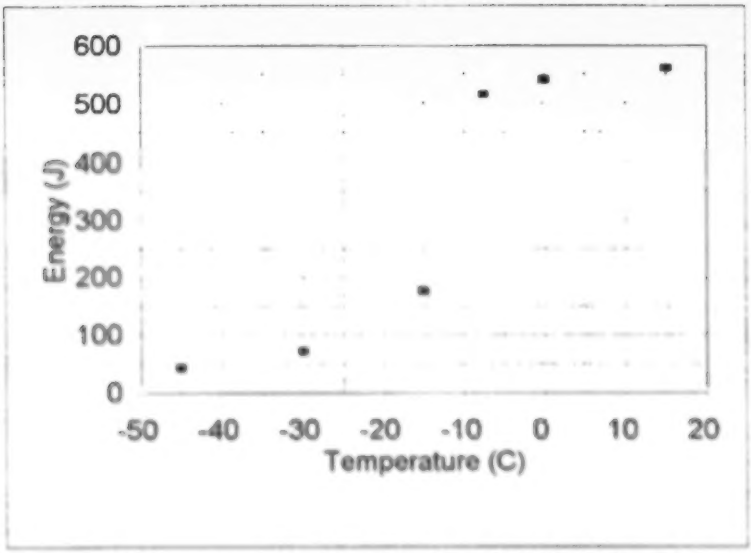


**Figure 8**- Temperature transition data for ASTM E-604 specimens precracked to .54 a/W with the notch oriented in the L-T orientation.

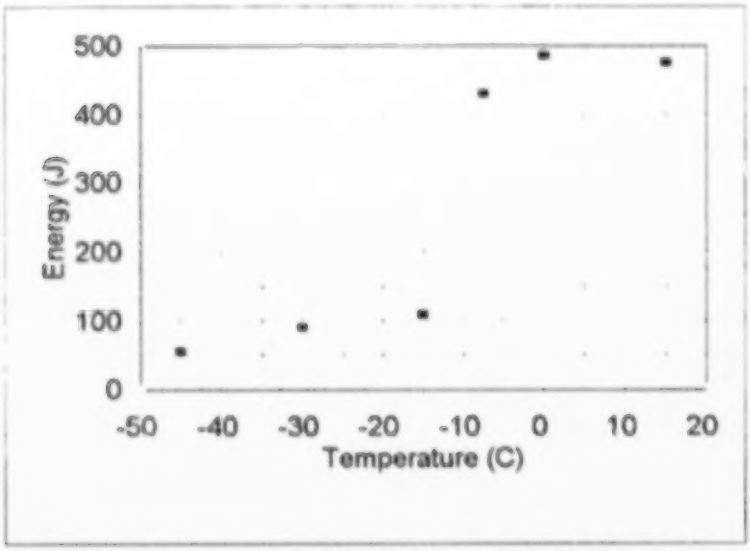


**Figure 9** - Temperature transition data for ASTM E-604 specimens precracked to 0.54 a/W with the notch oriented in the T-L orientation.

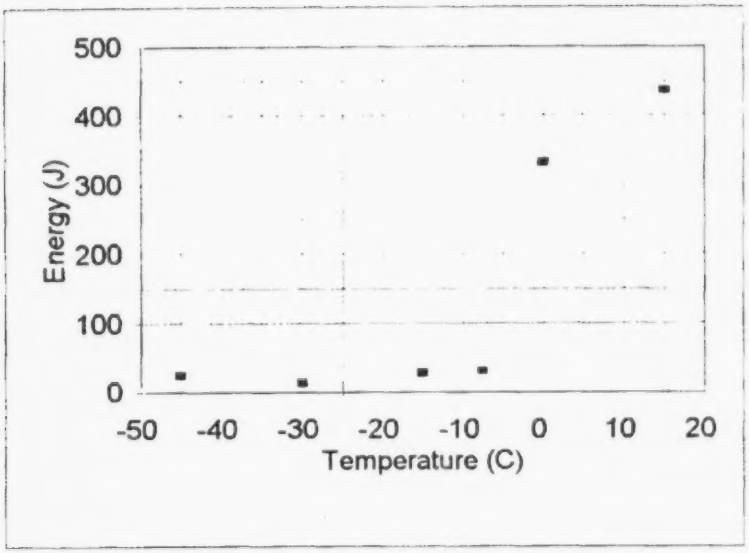


**Figure 10** - Transition data for ASTM E-604 specimens side grooved to 20 percent of the specimen thickness and precracked to .54 a/W. The notch for these specimens was machined in the L-T orientation.

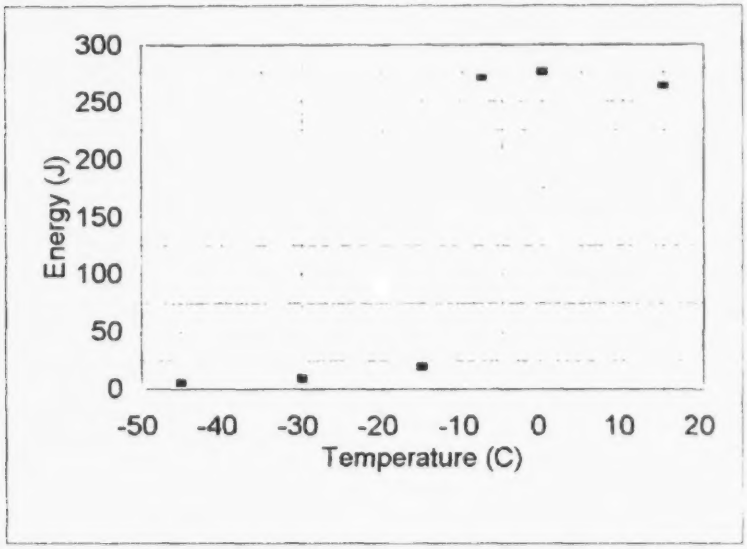


**Figure 11** - Transition data for specimens side grooved to 20 percent of the specimen thickness and precracked to .54 a/W. The notch for these specimens was machined in the T-L orientation.

## 5.0 Discussion

It has been shown that the initial loading response of the specimen is dominated by the transfer of inertial energy from the striker to the specimen. The measured peak loading and absorbed energy during this event agree with simple force and absorbed energy calculations representing the theoretical magnitudes. This agreement indicates that total absorbed inertial energy is dependent on only the mass of the specimen and the initial striker velocity. Thus energy magnitudes below the total impulse energy would mask the specimen material/geometry response to the three-point bending loading response of the test. Owing to the relatively small contribution of energy from inertial sources to the total absorbed upper shelf energy for most metallic materials, the inclusion of this energy in total absorbed energy for the qualitative assessment of a transition temperature should not significantly influence the results. However, for the quantitative assessment of materials parameters such as initiation toughness, removal of the inertial energy from initiation energy would be prudent and at worst would result in a conservative estimate of fracture toughness levels.

The introduction of a compressive residual stress field at the tip of the pressed notch E-604 specimen may contribute significantly to the differing morphology of the fracture surface in the form of out of plane fracture observed for the side-grooved pressed-notched specimens. Pressing the notch of the E-604 specimen with a 0.025 mm radius knife to a depth of 0.010 in results in an applied mode I tension stress for the notch tip material during the press. Local crack tip stresses at peak knife deflection are well above the plastic flow stress of the material [2]. Upon removal of the knife, the result is a sharp pseudo crack at the notch tip which is surrounded by a zone of compressive residual stress, the magnitude of which is on the order of the yield stress of the material. Thus, upon testing the specimen in three-point bending, the actual stress field in advance of the crack tip is the combination the mode I stress field applied through specimen deflection and the compressive residual stresses present in the specimen as a result of pressing the notch. In the centre of the crack plane (plain strain) location, the lateral constraint will have the effect of increasing the resulting compressive residual stress over the lateral free surfaces. It has been observed that subsequent to pressing the notch, lateral distortion of the material at the notch tip free surface is evident. The super position of the increased stress generated at the lateral free surfaces through the introduction of side grooves combined with the increase in applied stress intensity factor required to initiate a brittle instability in the plain strain (centre of the crack plane promotes fracture initiation at the side-groove and notch-plane intersection. The out of plane fracture observed is consistent with the planes of maximun shear imposed by the side grooves.

It has been postulated in the background section that a topic which has received little study and may provide significant input with respect to accounting for a portion of the transition temperature differences observed between specimens of differing geometry is the effect of the temperature increase at the crack tip owing to plastic strain converted into heat in the plastic zone. For a precracked specimen, an idealized first order approximation of plastic zone size ($r_y$) for plain strain conditions is given by the Von Mises criterion [17] as:

$$r_y = \frac{1}{6\pi}\left(\frac{K_I}{\sigma_{ys}}\right)^2 \qquad (5.1)$$

where ($K_I$) is the applied stress intensity and ($\sigma_{ys}$) is the material yield stress. For plain strain, the elastic stress intensity factor ($K_I$) can be approximated from the relationship in ASTM E399 [16] as:

$$K_I = \frac{PS}{BW^{3/2}} f\left(\frac{a}{W}\right) \qquad (5.2)$$

where (P) is the applied load, (S) is the specimen span, (B) is the specimen thickness, (W) is the specimens height, and f(a/W) is a multiplication factor dependent on precrack depth. Thus, if the average post inertial loading (prior to crack initiation) is substituted into equations 5.1 and 5.2 for the precracked L-T specimen shown in Figure 4.1, the plastic zone corresponding to this applied load can be calculated as approximately 1.88 mm. Thus the total volume for the plastic zone in this specimen is calculated as 73.7 $mm^3$. The plastic strain sustained by the specimen prior to the initiation of the brittle instability is measured as the difference of total energy to initiation minus inertial impulse energy which in this case of Figure 4.1 is approximately 4.1 J. Given that the heat capacity of steel is approximately 0.448 J/g.°C and assuming complete conversion of the plastic strain into heat, the increase in plastic zone material temperature is approximately 1.5 °C. This would suggest that the critical temperature for the susceptibility of this material to a transgranular cleavage event is approximately -13.5°C. For the L-T pressed notch E-604 specimen, the measured absorbed energy difference of total initiation energy minus inertial energy is approximately 29.7 J. If the critical plastic zone size to initiate a brittle instability in this specimen is assumed to be approximately equal to that of the precracked specimen, calculation of the plastic zone temperature increase owing to the conversion of plastic strain into heat results in a temperature increase of approximately 11.25 °C. This would suggest that the critical temperature for the susceptibility of this material to a transgranular cleavage event is approximately -13.75°C . The agreement between the material susceptibility temperature between the pressed notch specimen to that predicted by a similar analysis on the precracked specimen indicates that crack tip heating owing to plastic zone heat conversion may significantly influence the apparent transition temperature as predicted by a particular specimen geometry. While the evidence presented in this report is by no means exhaustive, it does indicate that this method of determining a geometry independent transition temperature does warrant further investigation.

## 5.0 CONCLUSIONS

Several inferences are generated from the data and analysis generated during this study. These inferences include:

1. The initial loading response of an instrumented impact system is dominated by the transfer of inertial energy from the striker to the specimen. Measured magnitudes of peak inertial loading and absorbed energy are in good agreement with theoretical values calculated from simple force and kinetic energy equations. Absorbed inertial energy is independent of the three-point bending response of the specimen. Thus, while inclusion of this energy in absorbed impact energy for qualitative procedures such as the development transition temperatures will have minimal influence on the predicted temperatures, quantitative procedures such as the determination of material initiation toughness should remove this energy from the analysis.

2. The out of plane fracture morphology observed for the side-grooved pressed notch specimens is attributed to the crack closure effects (notch tip compressive residual stresses) introduced into the ASTM E-604 specimen as a result of the pressing of a sharpened knife into the notch prior to conducting the test. The global effect of the compressive notch tip stress was the promotion of initiating the fracture event at the specimen lateral surfaces.

3. ASTM E-604 and precracked specimen geometries were used to generate temperature transition curves for CSA-G40.21 350WT structural steel. Transition curves for notch configurations were generated for T-L and L-T notch orientations with and without side-grooves. It was observed that within a specific specimen geometry, both T-L and L-T notch orientations produced similar transition temperatures. The out of plane fracture observed in the side grooved pressed notch E-604 specimen produced non-representative transition curves as compared to the other specimen geometries tested and thus is not recommended for transition curve analysis. The transition temperatures predicted by the non-side-grooved precracked and non-side-grooved pressed-notch geometries were approximately -15°C and -25°C, respectively. These results indicated a small geometry dependence of the lower knee transition temperature of approximately 10°C between these two geometries.

4. A framework for adjusting material temperature transition curves has been described. The framework proposed the adjustment of the temperature owing to conversion of plastic strain energy in the crack tip plastic zone into heat. Lower knee load-displacement records were used to analyse the magnitude of the temperature adjustment for both the precracked and pressed notch L-T 350 WT steel specimens. The analysis indicated that the material transition temperature as predicted was -13.75°C and -13.5°C for the ASTM E-604 pressed notch and precracked specimen, respectively. While, the analysis conducted into the validity of this framework is by no means exhaustive, the good agreement between the material transition temperature as predicted by the two specimen geometries studied is encouraging.

P518202.PDF [Page: 30 of 49]

## 6.0 REFERENCES

[1] "Standard Test Methods for Notched Bar Impact Testing of Metallic Materials," Annual Book of ASTM Standards, vol. 3.01, 1997.
[2] "Standard Test Method for Dynamic Tear Testing of Metallic Materials," Annual Book of ASTM Standards, vol. 3.01, 1997.
[3] "Standard Test Method for Drop-Weight Tear Tests of Ferritic Steels," Annual Book of ASTM Standards, vol. 3.01, 1997.
[4] "Standard Test Methods for Conducting Drop-Weight Test to Determine Nil-Ductility Transition Temperature of Ferritic Steels," Annual Book of ASTM Standards, vol. 3.01, 1997.
[5] Matthews, J.R., C.V. Hyatt and J.F. Porter, "Effect of Thickness on the Relationship Between Shear Lip and Energy in Dynamic Tear Specimens," Engineering Fracture Mechanics, vol. 60, no. 5-6.
[6] Matthew, J.R., E.J. Robichaud, V. Roy and C.V. Hyatt, "Dynamic Tear Structural Transition Determination for Steel and Weldments Removed from HMCS Calgary," DREA Note No. DL(A)/98/7.
[7] Sumpter, J., KarisAllen, K.J. et al,"TTCP Operating Assignment on Fracture Control of Naval Structures Report", Final Report, PTP/8/93, May 1993.
[8] Lesuer, D.R., "Experimental Investigations of Material Models for Ti-6Al--4V Titanium and 2024-T3 Aluminum", DOT/FAA/AR-00/25, Office of Aviation Research, Washington, DC.
[9] KarisAllen, K.J., "Quantitative Fracture Properties in the Transition Region and Near Transition Region for Thin Plate Ship Steel ", Final Report, Contract No. W7707-8-6321/001/HAL
[10] KarisAllen, K.J., "DREA DropTower Electronics Conversion," DREA Contractor Report, 1997.
[11] KarisAllen, K.J., "DREP Instrumented Impact Testing System," DREP Technical Memorandum 89-2.3 July 1989.
[12] KarisAllen, K.J., Rhyno, K.J., and Matthews, J.R., "Calibration of the DREA Drop Weight Instrumented Impact Testing System," DREA RN/DL/85/1, January 1985.
[13] Bhome, W. And Kalthoff, J.F., "The Behaviour of Notched Bend Specimens in Impact Testing", International Journal of Fracture, Vol 20, Dec. 1982. pp. R139-R143.
[14] KarisAllen, K.J. and Morrison, J., "Mechanical Reduction of Inertially Generated Effects in Single-Edge Notched Bend (SENB) Specimens Subjected to Impact Loading", Rapid Load Fracture testing, ASTM STP 1130, American Society for Testing and Materials, 1992, pp. 76-91.
[15]"Standard Test Methods for $J_{IC}$, A Measure of Fracture Toughness," Annual Book of ASTM Standards, vol. 3.01, 1997.
[16]"Standard Test Methods for Plane-Strain Fracture Toughness of Metallic Materials," Annual Book of ASTM Standards, vol. 3.01, 1997.
[17] Ewalds, H.L. and Wanhill, R.J.H., Fracture Mechanics" Edward Arnold Ltd, Australia 1984.

# Appendix A
# DREA Instrumented Impact Testing System

Software User Manual (Version 2)

P518202.PDF [Page: 32 of 49]

## A.1.0 SYSTEM DESCRIPTION

### A.1.1 Hardware Requirements

- IBM 586 compatible microprocessor
- SVGA terminal
- Microsoft compatible mouse
- 101 Enhanced keyboard
- Gage Applied Sciences Inc CSLITE (64K) A/D board
or a Gage Applied Sciences Inc CS225 (128K) A/D board
- Vishay 2300 Signal Conditioner/Amplifier

A schematic of the hardware interconnections is shown in Figure A.1. To configure the system hardware, connect the TUP cable to the back panel connector labelled INPUT on the Vishay 2311 signal conditioner/amplifier (for pin out specifications refer to the ETI and Vishay User Manuals). The CSLITE A/D and CS225 boards are installed into ISA slots on the PC 586 mother board and the back panel output BNC connector labelled TAPE on the Vishay 2311 is connected to the back panel connector labelled CH A (use a shielded BNC connector) on either the CSLITE or CS225 depending on the digitizing card required for testing.

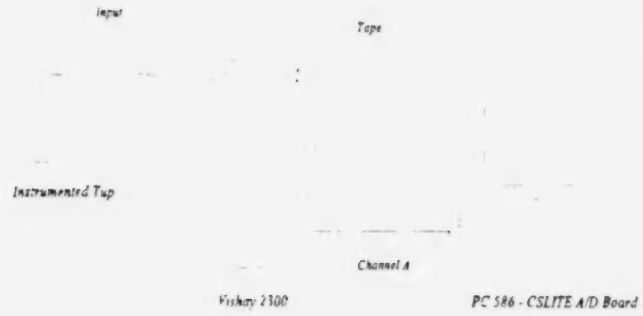


**Figure A.1** - Schematic representation of DREA instrumented impact test system hardware configuration.

A.1.2 Software Requirements

The software package consists of a single executable " DREADT2.EXE" and two dynamic link libraries "CW3215.DLL" and "GAGEDRV.DLL" which combine to generate a custom designed virtual instrument which executes the acquisition and analysis of impact force - time data. The system was designed for a 32 bit Windows 95/98 environment and will not execute properly in 16 bit environments such as DOS or Windows 3.1. If the custom software requires reinstallation, the following steps should be followed:

a) Insert the installation disk into drive A:

b) Enter the command A:INSTALL<CR> from the keyboard (this can be done from either DOS or Windows environments).

Once the software has been installed on the system, make sure that the data file "cal.txt" file contains the proper calibration factors. This file can be viewed/edited by clicking on the calibrate command in the software main menu header or by using a commercially available text editor (not a word processor).

A.1.3 Calibration Procedure

The instrumented impact system requires periodic calibration verification of the force transducer to ensure the accuracy of the data. This verification is achieved through one of the following static calibration procedures.

Procedure I

1. Attach the tup to the conditioner input and a voltmeter to the output of the conditioner as detailed in the System Description section.

2. Apply an axial compressive load to the instrumented tup using a calibrated servo hydraulic test system or comparable device.

3. Record the calibrated load versus the output voltage at a minimum of ten positions over the full scale range. Plot the data and visually verify the linearity of the force-voltage output.

4. Determine the calibration coefficient in units of kN/volt

5. Repeat steps 2-4 for each system amplifier range/excitation voltage combination used by the system.

6. Update the "cal.txt" file located in the system root directory with the current

P518202.PDF [Page: 34 of 49]

calibration coefficients or by entering the new calibration factors using the calibrate main menu command in the system software.

Procedure II

An alternative method of generating the calibration factors required is to generate the calibration factor for a single load range (steps 1-4 in procedure I) where the gain and transduce excitation voltage are accurately known. From this information the calibration factor associated with any other combination of gain and excitation voltage can be calculated using the relationship:

$$CF_{calc} = \frac{CF_m \cdot Ex_{calc} \cdot G_{calc}}{Ex_m \cdot G_m} \qquad (9)$$

where $Ex_{calc}$ and $G_{calc}$ are the excitation voltage associated with the calculated calibration factor to be calculated and $Ex_m$ and $G_m$ are the excitation voltage associated with the experimentally measured calibration factor $CF_m$.

Using procedure I, a series of typical calibration factors representing various load ranges are given in Table A.1 and shown graphically in Figure A.2. The raw data used as input and the results of the regression analysis is given in Section A.5.

**Table A.1** - Typical system calibration factors

| Instrument ID | Calibration Factor (kN/Volt) | Full Scale Load Range (kN) | Amplifier Excitation Voltage (Volts) | Amplifier Gain |
|---|---|---|---|---|
| E5/G10 | 624.86 | 624.86 | 5.0 | 10 |
| E1/G100 | 318.00 | 318.00 | 1.0 | 100 |
| E2.7/G100 | 117.01 | 117.01 | 2.7 | 100 |
| E5/G100 | 63.89 | 63.89 | 5.0 | 100 |

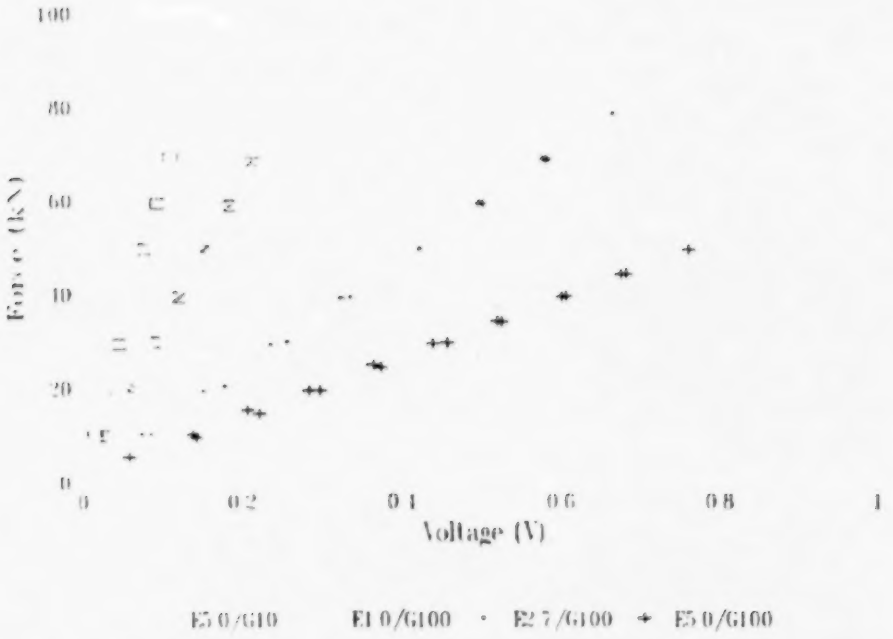


**Figure A.2** - Calibration curves (force versus voltage) for the four system transducer ranges.

As prescribed in ASTM E-04, transducer verification/calibration should be performed once a year. If the calibration coefficients vary more than 1% from the previous calibration coefficients, then this period should be decreased to 6 months. Also, the Vishay 2311 automatically monitors the resistances in the force transducer. If gauge resistances are mismatched between 1%-5%, the yellow HI LED will be activated. If the gauge resistances are mismatched by more than 5%, the yellow HI LED blinks indicating a serious transducer problem. Changes in transducer resistances indicate a need for an immediate recalibration of the system.

## A.2.0 GETTING STARTED

The DREA instrumented impact testing system is a R&D oriented software package designed for gathering and analysing dynamic force time data. Once the system has been configured, data base generation and maintenance is self supervising. Using this system requires no previous experience with computers. The system has a single control display which allows the operator complete access to the program functions. To initiate the program and generate the control display, choose the DT2001 icon from the Windows desktop.

A bitmap of the user interface associated with this program is shown in Figure A.3. The display is divided into four sections. The column of windows located on the left hand side of the display are for the input of client, test apparatus, test specimen, and procedure description. While these variables do not effect the acquisition of the data, several are used for post processing the data from load/time to load/displacement. The variables associated with these windows can be up to 100 characters long. The initial screen displays the data types associated with each of the windows.

The bottom centre/right section of the screen contains various check boxes, scroll bars and track bars which are used to set up and control the digitizer during data acquisition. The operator can set test parameters such as digitizer selection, transducer range, digitizing rate, trigger level and the trigger delay. The system has been preprogrammed with valid CSLITE and CS225 settings to minimize operator error during digitizer setup (see Table A.2 for available settings).

Table A.2 - Available Digitizer Settings

| Parameter | Available Settings | |
|---|---|---|
| | CSLITE | CS225 |
| Voltage Range | ±1Vdc | ±5Vdc |
| Digitizing Rate | 1-2-5-10-20 µs/point | 1-2-5-10-20 µs/point |
| Trigger Level | ±1Vdc | ±5Vdc |
| Trigger Delay | 1-2000 points | 1-2000 points |

The upper centre/right section of the screen contains the check boxes and track bars used to activate data capture and control post processing of the data display located immediately below these controls. Using the track bar and displayed graphic cursor, the operator can define the point of initial impact ("Start" button) and final fracture ("End" button). In a similar fashion, the data can also be scanned by the operator using the cursor option. A scroll box containing the engineering values of the data pointed to by the graphic cursor can be viewed by activating the "Edit On" radio button located in the upper left hand corner of the display.

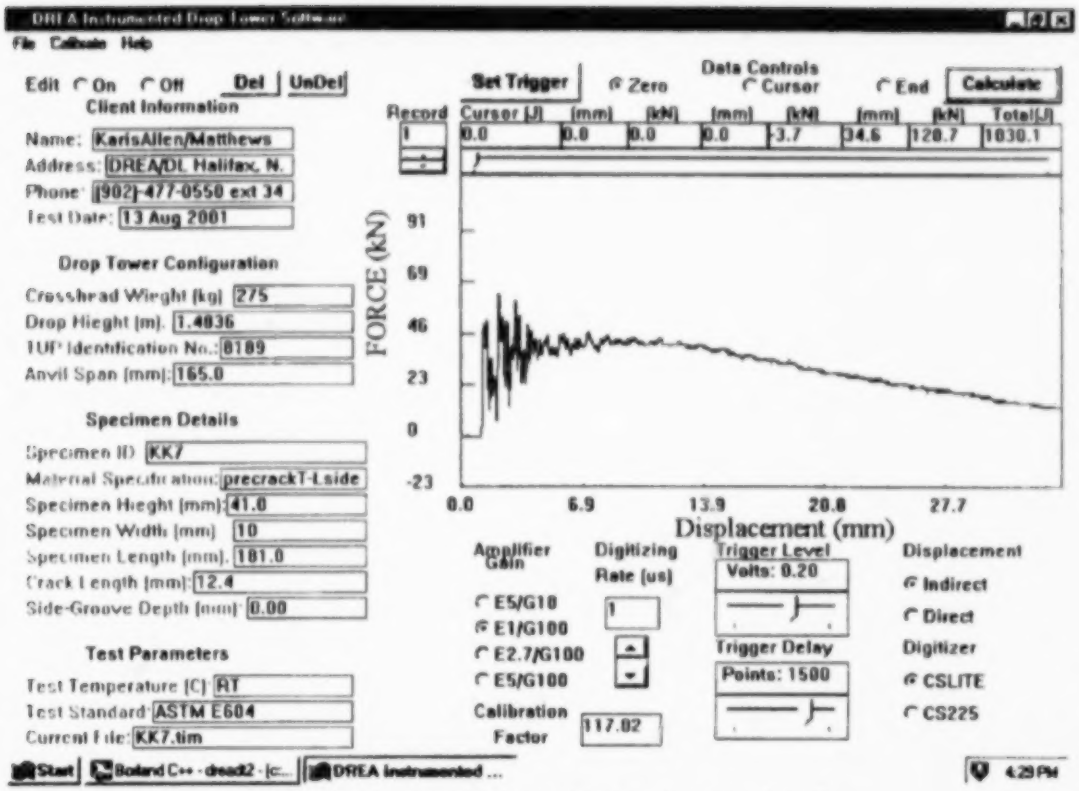


**Figure A.3** - Bitmap of DREA instrumented impact test system user interface.

The final section of the display is the command menu located along the top of the display. The command menu allows the operator to input variables from ASCII text files as well as output captured data to either ASCII text files or to a hardcopy device such as a printer or plotter. The following sections detail data input, data capture/post processing and data output.

### A.2.1 Inputting Test Variable Parameters

There are two methods available for inputting configuration data to the system. Upon system initialization, the user can manually enter data into the description variables and digitizer control buttons. Alternatively, if a variable data file was saved previously "ID.tim"(section A.2.4), then this file can be recalled to automatically configure the system to the previously saved configuration. The basic procedure for inputting a file is given as:

a) Choose FILE/OPEN from the command menu.
b) Click on the name of the file to be opened.
c) Click on OK box in the Open File window box.

Regardless of the manner in which the system is configured, the system should now be ready for data capture.

### A.2.2 Data Capture and Post Processing

Once the system has been properly configured (see section A.2.1), the digitizer can be activated by clicking on the "SET TRIGGER" button. The system will remain activated for 20 seconds. Version 2.0 of the software has been configured to capture multiple waveforms. Immediately upon filling the 8K data buffer, the system will rearm itself for any subsequent valid triggering event. The system is capable of capturing up to eight 8K waveforms. Upon timing out after 20 seconds, a message is displayed providing the number of waveforms captured. If the trigger condition times out with out encountering a valid triggering event, a message to this effect will appear on the screen. If multiple triggers have occurred, the operator can view individual waveforms by either incrementing or decrementing the "Records" scroll bar located at the upper left corner of the data display box. ***Immediately upon the successful capture and viewing of the desired impact trace, save the file (section A.2.4) to avoid the possible loss of valuable data.***

Post processing of impact data is achieved using the "ZERO", "END", and "CALCULATE" buttons combined with the graph track bar located at the top of the graph (repositioning the graph track bar activates the data cursor located in the graph display box) . The point of impact can be selected by clicking on the "ZERO" button. Pulling the track bar pointer in combination with the keyboard arrow keys is used to isolate the position of initial impact. Accurately defining the point of initial impact is necessary in order to define the initial velocity conditions for the numerical algorithm which converts load/time to load/displacement using conservation of energy principles. The point of final fracture can be similarly defined by clicking on the "END" button and using the track bar and keyboard arrow keys. The system has data boxes to display force and displacement values associated with the zero and end positions. Engineering values associated with the position of the graphic cursor can be viewed by activating the "Edit On" button (section A.2.3).

### A.2.3 Viewing Waveform Data

Engineering values associated with the position of the graphic cursor can be viewed by activating the "Edit On" button located in the upper left corner of the display. The system is programmed to dynamically refresh the data box as the graphic track bar or the arrow keys reposition the graphic cursor. The data associated with the current graphic cursor position is highlighted with in the data display box.

The operator has also been provided with the option to remove unrepresentative data from the waveform. With the "Cursor" and "Edit On" buttons activated, the data point associated with the position of the graphic cursor position can be deleted by clicking on the "Delete" button. The system can also reinsert the last point deleted by clicking the "Undelete" button. The system is capable of deleting and undeleting up to 100 individual data points per waveform.

### A.2.4 Saving and Printing Data

There are two different types of files which the operator can save to disk storage. File structures for these different types of files are given in Section A.4. The first type and probably the most commonly saved type of file is the load/time data file. Saving load/time data is done immediately after the successful capture of a new instrumented impact record. This file is saved using the ".tim" file descriptor (the "*.tim"file type is the default setting). If the operator requires a data file containing load/displacement couplets for the displayed data, this can be achieved by saving the file using the ".lpd" file descriptor (adjust the file type list to the "*.lpd"). This data file type can be imported into most commercially available spreadsheet and graphing packages. The basic procedure for saving a file is the same regardless of file type. This is given as:

a) Choose FILE/SAVE from the command menu.
b) Set the file type using the file type menu.
c) Input the name of the file to be saved (include the file descriptor).
d) Click on OK box in the Save File window box.

A hardcopy of the data currently being displayed can be obtained by choosing the FILE/PRINT option from the command menu.

## A.3.0 EXPERIMENTAL VERIFICATION OF INSTRUMENTATION

To provide an experimental verification of the accuracy of the system developed, 8mm thick specimens of CSA G40.21 350WT were tested in the L-T and T-L orientations. Dimensional measurements and tolerances in accordance with ASTM E-604 were observed. The three-point-bend specimens were impacted at 1.50 m/s with a 275 kg crosshead. The signal from the instrumented transducer was routed to the Vishay 2311 signal conditioner/amplifier. The amplified signal was routed from the amplifier to the 8 bit digitizer where the signal was captured and stored for subsequent analysis. Figures A.4 and A.5 are the load/displacement records for the L-T and T-L orientations, respectively. The total impact energy for the L-T orientation was 446 Joules while T-L impact energy was 247 Joules. Both these values were within the scatter associated with these previously characterized specimens.

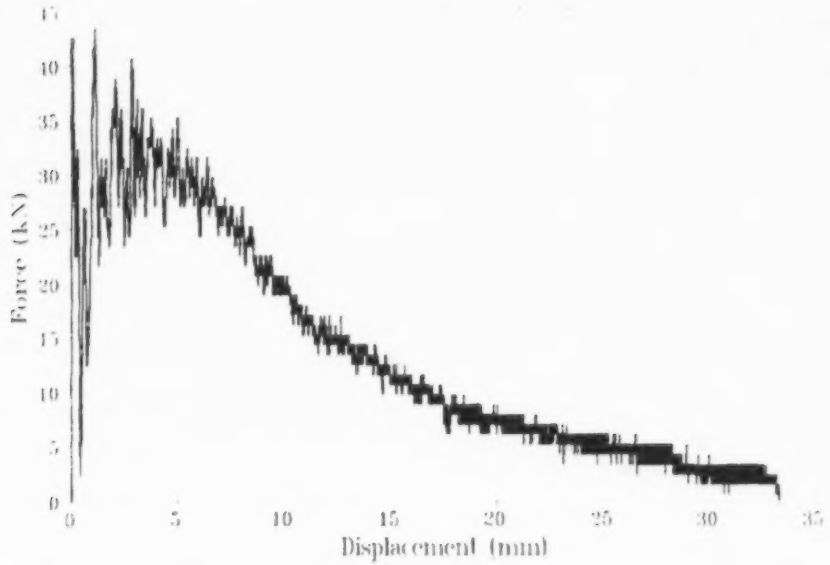


**Figure A.4** - Load/Displacement record for a 12 mm CSA G40.21 specimen in the L-T orientation impacted at 1.5 m/s.

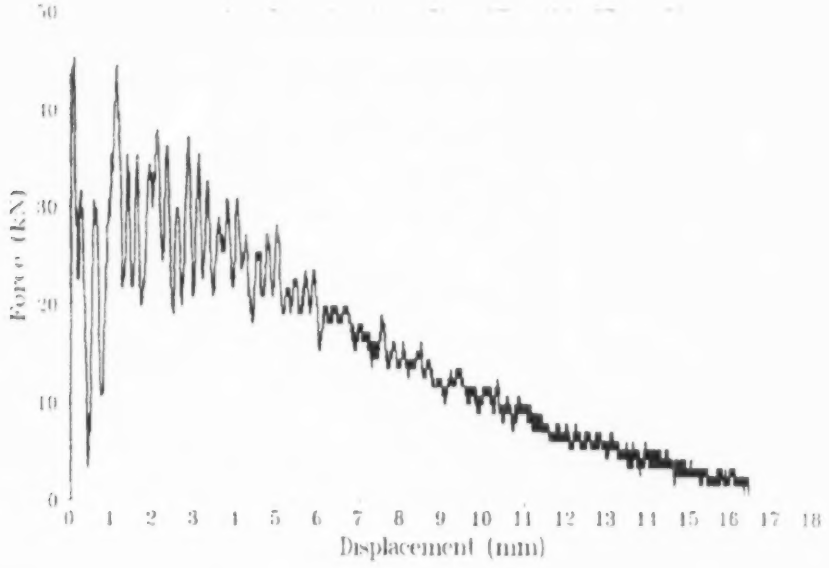


**Figure A.5** - Load/Displacement record for a 12 mm CSA G40.21 specimen in the T-L orientation impacted at 1.5m/s

**A.4.0 - File Structures**

A.4.1 Load/Time File

File Identification Code (variable file is 1001) <CR>
Name (text - max 100 characters) <CR>
Address (text - max 100 characters) <CR>
Phone No. (text - max 100 characters) <CR>
Test Date (text - max 100 characters) <CR>
Weight (float - kg) <CR>
Drop Height (float - m) <CR>
Tup ID (text - max 100 characters) <CR>
Anvil Span (float - mm) <CR>
Specimen ID (text - max 100 characters) <CR>
Material Spec (text - max 100 characters) <CR>
Specimen Height (float - mm) <CR>
Specimen Width (float - mm) <CR>
Specimen Length (float - mm) <CR>
Specimen Crack Length (float - mm) <CR>
Specimen Side Grooves (float - mm) <CR>
Temperature (text - max 100 characters) <CR>
Test Standard (text - max 100 characters) <CR>
Current File (text - max 100 characters)<CR>
Excitation/Gain (Integer - 1, 10, 100, 1000 - Excitation and gain set during calibration) <CR>
Calibration Factor (float - kN/volt) <CR>
Digitizing Rate (Integer - 1, 2, 5, 10, 20 - sweep time per point in microseconds) <CR>
Channel A Status (Integer - 0=OFF, 1=ON) <CR>
Channel B Status (Integer - 0=OFF, 1=ON) <CR>
Points in Trigger Delay (Integer - 0 to 2000) <CR>
Trigger Source (Integer - 0=Channel A, 1=Channel B) <CR>
Trigger Level (Integer - 0 to 255 represents -1.0V to 1.0V) <CR>
No. of Data Points in File (Integer) <CR>
Start Data String (char - 0 to 255) ..... End Data String (char - 0 to 255) <CR>
<EOF>

A.4.2 Load/Displacement File

File Name (File Name: Text) <CR>
Specimen ID (Specimen ID: text) <CR>
Total Energy (Total Energy: float - Joules) <CR>
Cursor Energy (Cursor Energy: float - Joules) <CR>
Start Selected Load/Displacement Data Interval (float - mm, float - kN) <CR>

.
.
.
.
.
.

End Selected Load/Displacement Data Interval (float - mm, float - kN) <CR>
<EOF>

**A.5.0 - Calibration Data**
(TUP Calibration (DREA/DL) Serial No. 07148)

A.5.1 Range 5VDC-X10

| Instron % FS (%) | Impact System (Volts) | Instron Force (kN) |
|---|---|---|
| 0 | -0.0029 | 0 |
| 10.8 | 0.0113 | 10.56845 |
| 19.3 | 0.0246 | 18.88621 |
| 29.8 | 0.0414 | 29.16109 |
| 40.4 | 0.0581 | 39.53382 |
| 50.4 | 0.0731 | 49.31942 |
| 60.5 | 0.0906 | 59.20288 |
| 70.4 | 0.1062 | 68.89062 |
| 79.9 | 0.1215 | 78.18694 |
| 70.8 | 0.108 | 69.28205 |
| 60.3 | 0.0913 | 59.00717 |
| 50.5 | 0.0766 | 49.41728 |
| 39.8 | 0.0598 | 38.94669 |
| 30 | 0.0446 | 29.3568 |
| 20.2 | 0.0289 | 19.76691 |
| 10 | 0.0136 | 9.7856 |
| 0 | -0.0031 | 0 |

Regression Output:

| | |
|---|---|
| Constant | 2.3348 |
| Std Err of Y Est | 0.838696 |
| R Squared | 0.998942 |
| No. of Observations | 17 |
| Degrees of Freedom | 15 |
| X Coefficient(s) | 624.8626 kN/Volt |
| Std Err of Coef. | 5.251049 |

A.5.2 Range 1VDC-X100

| Instron % FS (%) | Impact System (Volts) | Instron Force (kN) |
|---|---|---|
| 0 | -0.0031 | 0 |
| 10 | 0.0235 | 9.7856 |
| 20 | 0.054 | 19.5712 |
| 30.1 | 0.0851 | 29.45466 |
| 39.9 | 0.1172 | 39.04454 |
| 50.2 | 0.1485 | 49.12371 |
| 59.9 | 0.1794 | 58.61574 |
| 70 | 0.211 | 68.4992 |
| 80.6 | 0.2421 | 78.87194 |
| 69.4 | 0.2101 | 67.91206 |
| 60.1 | 0.1831 | 58.81146 |
| 50.9 | 0.154 | 49.8087 |

Regression Output:

| | |
|---|---|
| Constant | 1.349338 |
| Std Err of Y Est | 0.673723 |
| R Squared | 0.999311 |
| No. of Observations | 17 |
| Degrees of Freedom | 15 |
| X Coefficient(s) | 318.0095 kN/Volt |
| Std Err of Coef. | 2.155367 |

| | | |
|---|---|---|
| 40.1 | 0.1216 | 39.24026 |
| 30.4 | 0.0913 | 29.74822 |
| 20.7 | 0.0616 | 20.25619 |
| 9.8 | 0.0274 | 9.589888 |
| 0 | -0.0031 | 0 |

A.5.3 Range 2.7VDC-X100

| Instron % FS (%) | Impact System (Volts) | Instron Force (kN) |
|---|---|---|
| 0 | -0.0031 | 0 |
| 10.2 | 0.0717 | 9.981312 |
| 19.7 | 0.1488 | 19.27763 |
| 29.7 | 0.2331 | 29.06323 |
| 39.9 | 0.3209 | 39.04454 |
| 60.4 | 0.4954 | 59.10502 |
| 70.2 | 0.5792 | 68.69491 |
| 80.1 | 0.664 | 78.38266 |
| 70 | 0.5802 | 68.4992 |
| 60.3 | 0.5012 | 59.00717 |
| 50.5 | 0.4213 | 49.41728 |
| 40 | 0.334 | 39.1424 |
| 30.4 | 0.2538 | 29.74822 |
| 20.8 | 0.1754 | 20.35405 |
| 10.1 | 0.0828 | 9.883456 |
| 0 | -0.0022 | 0 |

| Regression Output | |
|---|---|
| Constant | 0.706496 |
| Std Err of Y Est | 0.698064 |
| R Squared | 0.9993 |
| No. of Observations | 16 |
| Degrees of Freedom | 14 |
| X Coefficient(s) | 117.0178 kN/Volt |
| Std Err of Coef. | 0.82774 |

A.5.4 Range 5VDC-X100 ;

| Instron % FS (%) | Impact System (Volts) | Instron Force (kN) |
|---|---|---|
| 0 | -0.0031 | 0 |
| 5.1 | 0.0561 | 4.990656 |
| 10.1 | 0.1358 | 9.883456 |
| 15.4 | 0.2043 | 15.06982 |
| 19.7 | 0.2819 | 19.27763 |
| 25.3 | 0.3621 | 24.75757 |
| 30 | 0.437 | 29.3568 |
| 34.9 | 0.5193 | 34.15174 |
| 40 | 0.5996 | 39.1424 |

| Regression Output | |
|---|---|
| Constant | 0.806491 |
| Std Err of Y Est | 0.541864 |
| R Squared | 0.998775 |
| No. of Observations | 20 |
| Degrees of Freedom | 18 |
| X Coefficient(s) | 63.89549 kN/Volt |
| Std Err of Coef. | 0.527481 |

| | | |
|---|---|---|
| 44.9 | 0.6749 | 43.93734 |
| 50.3 | 0.7611 | 49.22157 |
| 45.1 | 0.6804 | 44.13306 |
| 40.2 | 0.6052 | 39.33811 |
| 34.7 | 0.5241 | 33.95603 |
| 30.2 | 0.4553 | 29.55251 |
| 24.8 | 0.373 | 24.26829 |
| 19.6 | 0.295 | 19.17978 |
| 14.6 | 0.2193 | 14.28698 |
| 9.5 | 0.14 | 9.29632 |
| 0 | -0.002 | 0 |

## DOCUMENT CONTROL DATA

(Security classification of title, body of abstract and indexing annotation must be entered when the overall document is classified)

1 ORIGINATOR (the name and address of the organization preparing the document. Organizations for whom the document was prepared, e.g. Establishment sponsoring a contractor's report, or tasking agency, are entered in section 8.)

FACTS Engineering Inc.
P.O. Box 20039
Halifax, Nova Scotia, Canada, B3R 2K9

2 SECURITY CLASSIFICATION (overall security classification of the document including special warning terms if applicable)

UNCLASSIFIED

3 TITLE (the complete document title as indicated on the title page. Its classification should be indicated by the appropriate abbreviation (S,C,R or U) in parentheses after the title)

Evaluation of the Transition Properties of CSA 350WT and Modifying the DREA Instrumented Impact Testing System

4 AUTHORS (Last name, first name, middle initial. If military, show rank, e.g. Doe, Maj. John E.)

K.J. KarisAllen

| 5 DATE OF PUBLICATION (month and year of publication of document) | 6a NO. OF PAGES (total containing information. Include Annexes, Appendices, etc.) | 6b NO. OF REFS (total cited in document) |
|---|---|---|
| January 2002 | 35 (approx.) | 17 |

7 DESCRIPTIVE NOTES (the category of the document, e.g. technical report, technical note or memorandum. If appropriate, enter the type of report, e.g. interim, progress, summary, annual or final. Give the inclusive dates when a specific reporting period is covered)

CONTRACTOR REPORT

8 SPONSORING ACTIVITY (the name of the department project office or laboratory sponsoring the research and development. Include address.)

Defence Research Establishment Atlantic
PO Box 1012
Dartmouth, NS, Canada B2Y 3Z7

| 9a PROJECT OR GRANT NO. (if appropriate, the applicable research and development project or grant number under which the document was written. Please specify whether project or grant) | 9b CONTRACT NO. (if appropriate, the applicable number under which the document was written) |
|---|---|
| 1gh 36 | W7707-00-8893/001/HAL |

| 10a ORIGINATOR'S DOCUMENT NUMBER (the official document number by which the document is identified by the originating activity. This number must be unique to this document.) | 10b OTHER DOCUMENT NOs. (Any other numbers which may be assigned this document either by the originator or by the sponsor.) |
|---|---|
| | DREA CR 2002-006 |

11 DOCUMENT AVAILABILITY (any limitations on further dissemination of the document, other than those imposed by security classification)

( X ) Unlimited distribution
( ) Defence departments and defence contractors; further distribution only as approved
( ) Defence departments and Canadian defence contractors, further distribution only as approved
( ) Government departments and agencies; further distribution only as approved
( ) Defence departments; further distribution only as approved
( ) Other (please specify):

12 DOCUMENT ANNOUNCEMENT (any limitation to the bibliographic announcement of this document. This will normally correspond to the Document Availability (11). However, where further distribution (beyond the audience specified in (11) is possible, a wider announcement audience may be selected)

13. ABSTRACT (a brief and factual summary of the document. It may also appear elsewhere in the body of the document itself. It is highly desirable that the abstract of classified documents be unclassified. Each paragraph of the abstract shall begin with an indication of the security classification of the information in the paragraph (unless the document itself is unclassified) represented as (S), (C), (R), or (U). It is not necessary to include here abstracts in both official languages unless the text is bilingual)

Energy based temperature transition curves have been constructed for a CSA G40.21 350WT structural steel for several specimen geometries using the load-displacement data generated by an instrumented impact test system. Specimen geometries employed include standard pressed notched ASTM E-604 and ASTM E-604 specimens precracked to approximately 0.55 a/W with notch orientations in both the T-L and L-T orientation. The effects of machining side grooves into the lateral specimen faces for both notch geometries has also been evaluated. A framework for adjusting material temperature transition curves has been described. The framework proposed focuses on the adjustment of the transition temperature owing to conversion of plastic strain energy in the crack tip plastic zone into heat.

The results indicate that with the exception of the pressed-notched, side-grooved specimens, the data from the lower shelf (brittle) to the upper shelf (ductile) combine to generate typical transition curve morphologies. Visual examination of the fracture surfaces of the pressed-notched, side-grooved specimens revealed significant amounts of out of plane fracture. The out of plane fracture morphology observed for the side-grooved pressed-notch specimens has been attributed to the fracture event initiating at the specimen lateral surfaces . It was observed that within a specific specimen geometry, both T-L and L-T notch orientations produced similar transition temperatures. The transition temperatures predicted by the non-side-grooved precracked and non-side-grooved pressed-notch geometries were approximately -15°C and -25°C respectively. These results indicated a small geometry dependence of the lower knee transition temperature of approximately 10°C between these two geometries.

Lower knee load-displacement records were used to analyse the magnitude of the temperature adjustment for both the precracked and pressed notch L-T 350 WT steel specimens. The analysis indicated that the predicted geometry independent material transition temperature is -13.7°C and -13.5°C for the ASTM E-604 pressed notch and precracked specimen, respectively. While the analysis conducted into the validity of this framework is by no means exhaustive, the agreement between the material transition temperature as predicted by the two specimen geometries employed warrants further study.

14 KEYWORDS, DESCRIPTORS or IDENTIFIERS (technically meaningful terms or short phrases that characterize a document and could be helpful in cataloguing the document. They should be selected so that no security classification is required. Identifiers, such as equipment model designation, trade name, military project code name, geographic location may also be included. If possible keywords should be selected from a published thesaurus, e.g. Thesaurus of Engineering and Scientific Terms (TEST) and that thesaurus identified. If it not possible to select indexing terms which are Unclassified, the classification of each should be indicated as with the title)

Dynamic Tear
Impact Testing System
ASTM E604
Side Grooved Fracture Specimens
DT Transition Curves